

# Precipitation Climate Data Record

## 1. Intent of This Document and POC

**1a)** This document is intended for users who wish to compare satellite derived observations with climate model output in the context of the CMIP5/IPCC historical experiments. Users are not expected to be experts in satellite derived Earth system observational data. This document summarizes essential information needed for comparing this dataset to climate model output. References are provided at the end of this document to additional information.

Dataset File Name (as it appears on the ESGF):

**--to be added once file is accepted----**

**1b)** Technical point of contact for this dataset:

Soroosh Sorooshian, Center for Hydrometeorology and Remote Sensing (CHRS) at University of California Irvine, soroosh@uci.edu  
Olivier Prat, Cooperative Institute for Climate and Satellites-NC at North Carolina State University, olivier.prat@noaa.gov

## 2. Data Field Description

CF variable name, units:	<i>precipitation, pr, precipitation flux, kg m-2 s-1</i>
Spatial resolution:	<i>0.25 degree in latitude and longitude</i>
Temporal resolution and extent:	<i>Daily and monthly averaged, from 01/1983 to (delayed) present</i>
Coverage:	<i>Global (60°N-60°S)</i>

## 3. Data Origin

The Daily Precipitation PERSIANN-CDR product is to be generated for each time step by first estimating precipitation for each GridSat-B1 Infrared Window (IRWIN) file using the basic PERSIANN algorithm, which uses an artificial neural network (ANN) to convert the input IR data in degrees Kelvin into rain rate (RR) data in mm/hr. Each month of PERSIANN estimates is then bias corrected with monthly GPCP precipitation data and the final PERSIANN-CDR product results when those bias correct precipitation estimates are accumulated to daily. The final product is produced with bias corrections from the monthly GPCP v2.2 data set, so a month of data is processed at the same time. Figure 1 provides the overview for the Daily PERSIANN-CDR production system.

The precipitation product PERSIANN-CDR is generated using the two datasets described below:

1. Before being used as primary data, the infrared data gridded from GridSat-B1 is converted to a derived format before input into the ANN model. The primary data are archived at the NOAA National Center for Environmental Information (NCEI; previously the Climatic Data Center: NCDC). NOAA/NCEI maintains an historical archive of data from geostationary (GEO) satellites, compiled by the International Satellite Cloud Climatology Project (ISCCP). ISCCP B1 (available online at: <http://www.ncdc.noaa.gov/oa/rsad/isccpb1>), includes all-channel observations from a number of international GEO satellites including the Geostationary Operational Environmental Satellite (GOES) series, the European Meteorological satellite (Meteosat) series, the Japanese Geostationary Meteorological Satellite (GMS) series, and the Chinese Fen-Yung 2C (FY2) series.

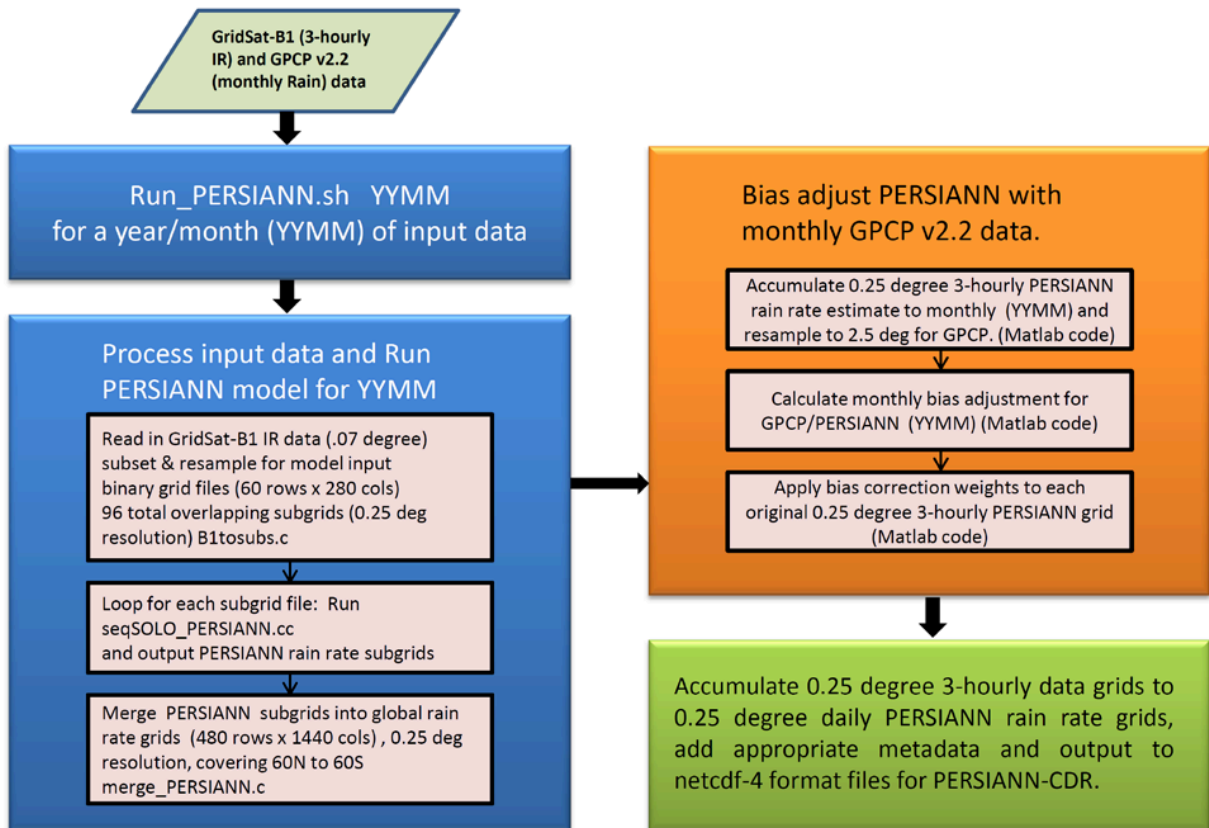


**Figure 1** DAILY PERSIANN-CDR production flowchart. Adapted from Hsu et al. (2014).

The global ISCCP B1 IR brightness temperature from these GEO sources covers the time period from 1979 to present, at space and time resolutions of 10-km and 3-hour intervals. Better coverage began in 1983, albeit with a gap over the Indian Ocean due to the lack of GEO measurements. Other sources, such as AVHRR (Advanced Very High Resolution Radiometer) from the NOAA series of satellites (NOAA-7~NOAA-14), can be used to fill part of the gap before 1997. Gridded Satellite (GridSat-B1) is the gridded derived product from ISCCP B1 data (available at: <http://www.ncdc.noaa.gov/oa/gridsat/index.php>). GridSat-B1 data provide data for three channels: visible data, infrared window (IRWIN) data, and infrared water vapor (IRWVP) data. The Infrared Window (IRWIN) data is the main input data for the PERSIANN model. The IRWIN data are gridded on a 0.07° latitude equal-angle grid. By selecting the nadir-most observations at each grid point, satellite data are merged. The IR window brightness temperature; identified as GridSat-B1 CDR (see Obs4MIPS technical note for more information) is used as primary data for PERSIANN-CDR. GridSat-B1 CDR starts from 1 January 1980 and continues to the current time. It covers the globe from 70°S-70°N and 180°W-180°E. The GridSat-B1 CDR data are available at <ftp://eclipse.ncdc.noaa.gov/pub/gridsat/b1-climate-data-record/>. Finally, in order to match the coarser PERSIANN-CDR resolution of 0.25°, the GridSat-B1 IRWIN data files are converted from their native resolution of 0.07° latitude/longitude to a 0.25° resolution in a flat binary format for input to the PERSIANN algorithm system. This

global coverage array is a 2-byte short integer binary format grid 480-rows by 1440-columns covering 60°N-60°S and 0°-360° longitude.

2. Monthly precipitation data from the Global Precipitation Climatology Project (GPCP) are used as ancillary data to correct for biases in the ANN model output. Briefly, GPCP was established in 1986 by the World Climate Research Program (WCRP) to document the spatial and temporal distribution of precipitation at climate scale (Adler et al. 2003). There are three GPCP global precipitation products available (version 2.2): (1) Monthly, 2.5° merged analysis (1979-present), (2) Pentad, 2.5° merged analysis (1979-present), and (3) Daily, 1° merged analysis (Oct. 1996-present). Briefly, the GPCP-v2.1 Monthly 2.5° merged analysis was constructed using multi-satellite (SSM/I and IR) precipitation estimates, adjusting the latter using gauge analysis to remove large-scale bias, and then merging satellite and gauge analysis into a final product (Huffman et al., 1997). The GPCP-v2.2 monthly product (available at <http://precip.gsfc.nasa.gov>) is the one used in the bias correction of the PERSIANN model output. More information on the GPCP v2.2 monthly precipitation product can be found at: [http://precip.gsfc.nasa.gov/gpcp\\_v2.2\\_comb\\_new.html](http://precip.gsfc.nasa.gov/gpcp_v2.2_comb_new.html).

The merging procedure for GridSat-B1 and GPCP v2.2 is performed according to the following steps:

1. Subset (96 overlapping subgrids) and resample (0.25° resolution) GridSat-B1 IR data (0.07° resolution) for ANN model input.
2. Run ANN model for each subgrid file and generate PERSIANN-B1 rain rate.
3. Merge PERSIANN-B1 subgrids into a global rain rate grid (0.25° resolution) covering 60°N-60°S (480 x 1140 grid cells). (Figure 2)
4. Accumulate PERSIANN-B1 3-hourly rain rate estimates to monthly accumulation.
5. Resample PERSIANN-B1 monthly accumulation to 2.5° resolution to match GPCP (Figure 2).
6. Calculate monthly bias adjustment coefficient  $w = \text{GPCP}/\text{PERSIANN-B1}$ .
7. Apply bias correction to each 3-hourly 0.25° PERSIANN-B1 pixel.
8. Accumulate each 0.25° 3-hourly pixel to 0.25° daily rain rate PERSIANN-CDR (Figure 2).
9. Add appropriate metadata and finalize output format to NetCDF-4 for PERSIANN-CDR.

Finally, in the context of Obs4MIPS and in order to facilitate Observation/Model intercomparison, the daily PERSIANN-CDR files are accumulated to create the monthly PERSIANN-CDR files so that both daily and monthly precipitation estimates are available. A conversion is made to convert the daily and monthly accumulations expressed in (mm/day) into a precipitation flux ( $\text{kg m}^{-2} \text{s}^{-1}$ ) more suitable for model intercomparison. The conversion from [mm/day] into [ $\text{kg m}^{-2} \text{s}^{-1}$ ] is made according to:

$$[\text{kg m}^{-2} \text{s}^{-1}] = [\text{mm/day}] \times [1000 \text{ kg/m}^3] \times [1/86400 \text{ day/s}] \times [1/1000 \text{ m/mm}] = [1/86400 \text{ mm/day}]$$

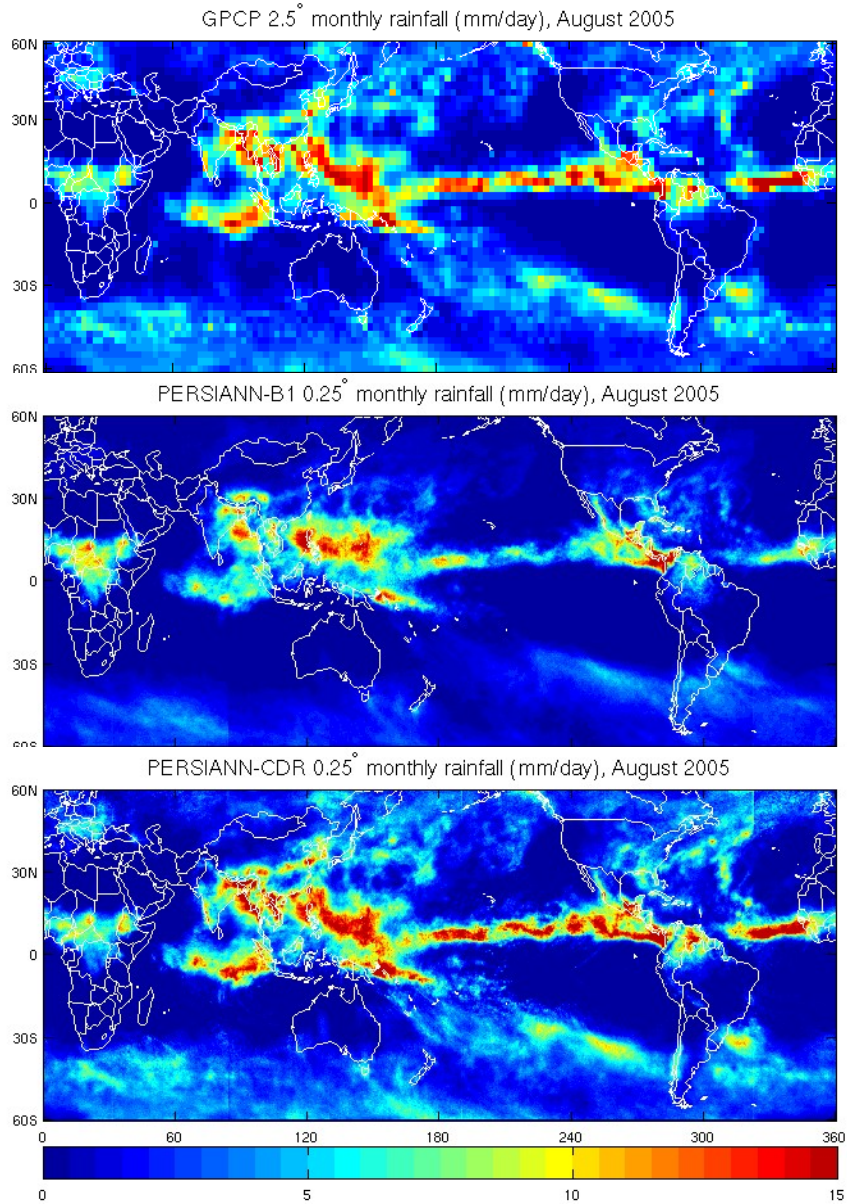


**Figure 2** Global average monthly rainfall maps ( $\text{mm day}^{-1}$ ) from (top) GPCP  $2.5^\circ$  (Adler et al. 2003), (middle) PERSIANN-B1  $0.25^\circ$ , and (bottom) PERSIANN-CDR  $0.25^\circ$  for August 2005. Adapted from Ashouri et al. (2005).

#### 4. Validation and Uncertainty Estimate

The ANN model forced with the GridSat-B1 IRWIN followed by the bias correction algorithm was evaluated over for 1983 to 2012. Figure 3 that displays the Mean Areal Precipitation (MAP) for Northern and Southern Tropical regions for GPCP, PERSIANN-B1, and PERSIANN-CDR shows that the GPCP precipitation dataset is correctly assimilated into the PERSIANN-CDR product, and that there is an adequate match between the PERSIANN-CDR and the GPCP datasets.

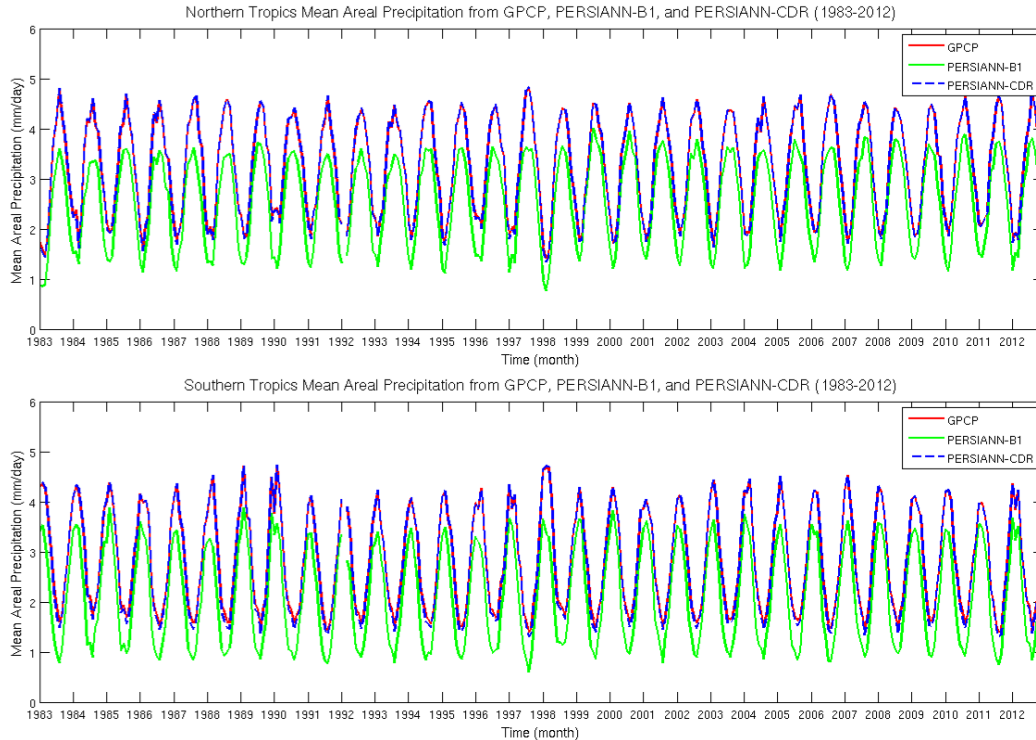


**Figure 3** Mean areal precipitation (mm/day) for Northern ( $0^{\circ}$ - $30^{\circ}$ N, top) and Southern ( $0^{\circ}$ - $30^{\circ}$ S, bottom) Tropics from monthly GPCP (red, Adler et al. 2003), PERSIANN-B1 (green), and PERSIANN-CDR (dashed blue) datasets. Adapted from Ashouri et al. (2015).

Further verifications were made at the daily scale between PERSIANN-CDR and GPCP-1DD (daily version of GPCP at  $1^{\circ}$  resolution starting 10/1996). Comparison performed over different areas (Global, Tropics, Northern Hemispheres, Higher latitudes), showed great consistency between PERSIANN-CDR and GPCP-1DD (Hsu et al. 2014).

In addition to elementary check of the algorithm stability and dataset consistency previously mentioned, the PERSIANN-CDR Daily dataset has been the focus of performance estimation against other products (satellite, radar, in-situ) and was used for various applications. The list of reference provides examples of those applications and of the validation against other products derived from satellites, radar, or in-situ data from local to global scales and various time scales. For instance, Ashouri et al. (2015) have compared PERSIANN-CDR with radar, gauges, and other satellites products for selected events (hurricane, extreme daily precipitation). The authors found globally comparable precipitation patterns with however significant local differences in term of rainfall accumulation. Further comparison with other satellite precipitation datasets showed similar long-term global daily averages and variability between the different products (Prat et al. 2014, 2015, 2016, Nelson et al. 2015). Differences between products were more important at the seasonal scale with respect to the location (N/S hemispheres) and when looking at extremes (Prat et al. 2016). A comparison with in-situ data showed overall consistent biases and correlations between products (Prat et al. 2016). Other validation of PERSIANN-CDR with satellite products and in-situ data have been conducted for domains over China and Central Asia (Guo et al. 2015a,b, Miao et al. 2015, Yang et al 2016, Yong et al. 2016, Zhu et al. 2016).

Although being primarily infrared (IR) based, PERSIANN-CDR was found to perform adequately with respect to rain gauge observations when compared to passive microwave (PMW) satellite products (Guo et al. 2015a,b). Better performance was found for PERSIANN-CDR during the cold season (Guo et al. 2015a), while lower performance was observed with respect to PMW products during Typhoon season (Yong et al. 2016). A limitation between most satellite products concerns the detection of light rainfall (Guo et al. 2015b). Although relatively satisfying, the performance in the detection of extreme precipitation events depends of the area considered and is lower over regions of complex topography (Miao et al. 2015).

## 5. Considerations for Model-Observation Comparisons

One point to take into consideration concerns the coverage of the primary sensor data GRIDSATD-B1 (Figure 4). Due to GRIDSAT coverage some PERSIANN-CDR daily files can have missing data over certain locations for the earlier years of the entire period of record. However, the PERSIANN-CDR entire period of record starting 01/1982 that is at a time where coverage was relatively satisfying the lack of coverage is limited to portions of the Indian Ocean. Furthermore, the inter-comparison of PERSIANN-CDR with other multi-satellite precipitation products, radar and in-situ datasets (Prat et al. 2014, 2015, 2016) indicate that this may have only a limited impact on the products accuracy at the daily scale or almost non-existent at the monthly scale.

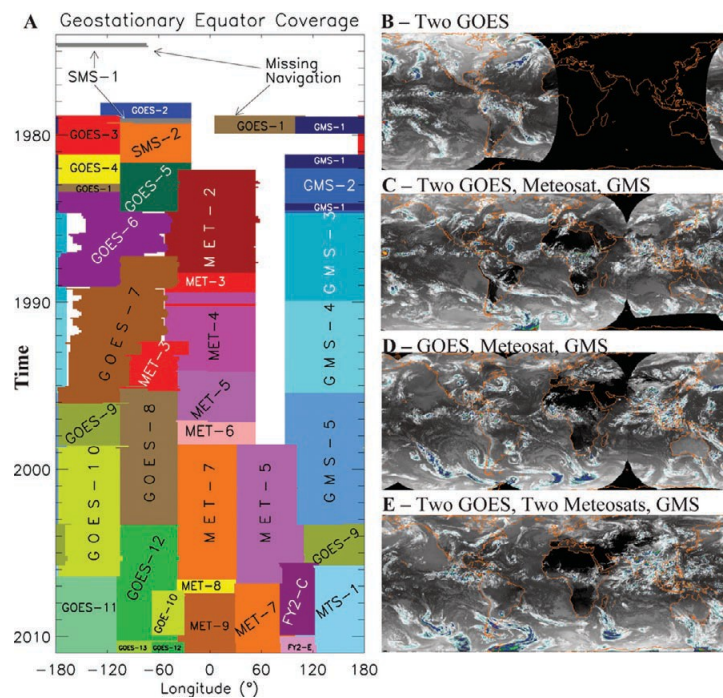


**Figure 4** (a) Time series of ISCCP B1 geostationary satellite coverage at the equator (limited to a view zenith angle of  $60^\circ$  for illustrative purposes). (b)-(e) Sample GridSat coverage for typical satellite coverages: (b) two-satellite coverage with only GOES-East and -West in 1980, (c) four-satellite coverage that is typical of most of the period 1982–98, (d) typical three-satellite coverage when the United States was operating only one satellite (1985-87 or 1989-92), and (e) five-satellite coverage that is typical of the current era (1998-present). Adapted from Knapp et al. (2011).

Another point to take into consideration is the spatial resolution of the final PERSIANN-CDR (see Figure 2). While the native resolution of PERSIANN-B1 is 0.25°, the calibration using lower resolution GPCP at 2.5° resolution tends to smooth the precipitation features within each 0.25° pixels with respect their neighboring counterparts in the final PERSIANN-CDR product with respect to PERSIANN-B1 or comparable satellite merged precipitation products (Prat et al. 2016).

## 6. Instrument Overview

The primary input data for the PERSIANN-CDR algorithm comes from another CDR: Gridded Satellite Data from ISCCP B1 (GridSat-B1) IR Window Channel. The GridSat-B1 data are combined from the various geostationary satellites available over the years from 1980-present. The infrared (IR) data from the imager instruments on board these satellites varies in wavelength but should be approximately 10.0 - 12.0µm. The GridSat-B1 data set merges and calibrates these inputs to provide the best available near global coverage (70°N to 70°S) for every 3 hour time step (Knapp et al. 2011).

The other input data is the Global Precipitation Climatology Project (GPCP) v2.2 2.5° monthly precipitation analyses derived from both satellite and ground data sources (Adler et al. 2003).

## 7. References

### Principal Publications of Dataset Description and Methodology

Ashouri, H, K. Hsu, S. Sorooshian, D. Braithwaite, K.R. Knapp, L.D. Cecil, B.R. Nelson, and O.P. Prat, 2015. PERSIANN-CDR: Daily precipitation climate data record from multi-satellite observations for hydrological and climate studies. *Bulletin of the American Meteorological Society*. 96, 69-80, doi:10.1175/BAMS-D-13-00068.1. Available at: <http://journals.ametsoc.org/doi/abs/10.1175/BAMS-D-13-00068.1>

Hsu, K., H. Ashouri, H. D. Braithwaite, and S. Sorooshian, 2014. PERSIANN-CDR C-ATBD. CDRP-ATBD-0286, 30pp. <http://www1.ncdc.noaa.gov/pub/data/sds/cdr/CDRs/PERSIANN/AlgorithmDescription.pdf>

### Publications on PERSIANN-CDR Dataset Ancillary Data

Adler, R., Huffman, G.J., Chang, A., Ferraro, R., Xie, P.-P, Janowiak, J., Rudolf, B., Schneider, U., Curtis, S., Bolvin, D., Gruber, A., Susskind, J., Arkin, P., and Nelkin, E., 2003. The version-2 Global Precipitation Climatology Project (GPCP) monthly precipitation analysis (1979–present). *Journal of Hydrometeorology*., 4, 1147-1167, doi:10.1175/1525-7541(2003)0042.0.CO;2.

Huffman, G.J., Adler, R.F., Arkin., P., Chang, A., Ferraro, R., Gruber, A., Janowiak, J., McNab, A., Rudolf, B., and Schneider, U., 1997. The Global Precipitation Climatology Project (GPCP) Combined Precipitation Dataset. *Bulletin of the American Meteorological Society*, 78, 5-20, doi:10.1175/1520-0477(1997)078<0005:TGPCPG>2.0.CO;2

Knapp, K.R., Ansari, S., Bain, C.L., Bourassa, M.A., Dickinson, M.J., Funk, C., Helms, C.N., Hennon, C.C., Holmes, C.D., Huffman, G.J., Kossin, J.P., Lee, H.-T., Loew, A., and Magnusdottir, G., 2011. Globally gridded satellite observations for climate studies. *Bulletin of the American Meteorological Society*, 92, 893-907, doi:10.1175/2011BAMS3039.1.

Presentations on Dataset Validation and/or Uncertainties (CICS-NC/NCEI)

- Nelson, B.R., O.P. Prat, and L. Vasquez, 2015. Precipitation Climate Data Records. *2015 AGU fall meeting*, December 14-18 2015, San Francisco, CA, USA.
- Prat, O.P., B.R. Nelson, E. Nickl, R. Adler, R. Ferraro, S. Sorooshian, and P. Xie, 2016. Global Evaluation of Satellite Based Quantitative Precipitation Estimates (QPEs) from the Reference Environmental Data Records (REDRs). *2016 EGU general assembly*, April 17-22 2016, Vienna, Austria.
- Prat, O.P., B.R. Nelson, S.E. Stevens, E. Nickl, and L. Vasquez, 2015. Toward the development of an evaluation framework of climate data records for precipitation. *2015 NOAA Climate Data Record (CDR) Program Annual Meeting*, August 3-7 2015, Asheville, NC, USA.
- Prat, O.P., B.R. Nelson, L. Vasquez, R. Ferraro, S. Rudlosky, and J.J. Wang, 2014. Evaluation of satellite based Quantitative Precipitation Estimates (QPEs) over CONUS (2002-2012): Comparison with surface and radar precipitation datasets. *7th Workshop of the International Precipitation Working Group (IPWG)*, November 17-21 2014, Tsukuba, Japan.

Publications on Dataset Validation and/or Uncertainties (non-CICS-NC/NCEI)

- Guo, H., Chen, S., Bao, A., Hu, J., Gebregiorgis, A.S., Xue, X. and Zhang, X., 2015a. Inter-comparison of high-resolution satellite precipitation products over Central Asia. *Remote Sensing*, 7(6), 7181-7211.
- Guo, H., Chen, S., Bao, A., Hu, J., Yang, B. and Stepanian, P.M., 2015b. Comprehensive evaluation of high-resolution satellite-based precipitation products over China. *Atmosphere*, 7(1), 6.
- Miao, C., Ashouri, H., Hsu, K.L., Sorooshian, S. and Duan, Q., 2015. Evaluation of the PERSIANN-CDR daily rainfall estimates in capturing the behavior of extreme precipitation events over China. *Journal of Hydrometeorology*, 16(3), 1387-1396.
- Yang, X., Yong, B., Hong, Y., Chen, S. and Zhang, X., 2016. Error analysis of multi-satellite precipitation estimates with an independent raingauge observation network over a medium-sized humid basin. *Hydrological Sciences Journal*, 61(10), 1813-1830.
- Yong, B., Wang, J., Ren, L., You, Y., Xie, P., and Hong, Y. 2016. Evaluating Four Multisatellite Precipitation Estimates over the Diaoyu Islands during Typhoon Seasons. *Journal of Hydrometeorology*, 17(5), 1623-1641.
- Zhu, Q., Xuan, W., Liu, L. and Xu, Y.P., 2016. Evaluation and hydrological application of precipitation estimates derived from PERSIANN-CDR, TRMM 3B42V7, and NCEP-CFSR over humid regions in China. *Hydrological Processes*. In Press. DOI: 10.1002/hyp.10846.

Publications with PERSIANN-CDR Dataset Applications or Citations (on 10 July 2016)

- Ashouri, H., Nguyen, P., Thorstensen, A., Hsu, K.L., Sorooshian, S. and Braithwaite, D., 2016. Assessing the efficacy of high-resolution satellite-based PERSIANN-CDR precipitation product in simulating streamflow. *Journal of Hydrometeorology*, in press.
- Ashouri, H., Sorooshian, S., Hsu, K.L., Bosilovich, M.G., Lee, J., Wehner, M.F. and Collow, A., 2016. Evaluation of NASA's MERRA precipitation product in reproducing the observed trend and distribution of extreme precipitation events in the United States. *Journal of Hydrometeorology*, 17(2), 693-711.
- Beck, H.E., van Dijk, A.I., Levizzani, V., Schellekens, J., Miralles, D.G., Martens, B. and de Roo, A., 2016. MSWEP: 3-hourly 0.25° global gridded precipitation (1979–2015) by



- merging gauge, satellite, and reanalysis data. *Hydrol. Earth Syst. Sci. Discuss., In Review*. doi:10.5194/hess-2016-236.
- Cassé, C., and M. Gosset, 2015. Analysis of hydrological changes and flood increase in Niamey based on the PERSIANN-CDR satellite rainfall estimate and hydrological simulations over the 1983-2013 period. *Conference: Symposium on Changes in Flood Risk and Perception in Catchments and Cities, Prague, CZ, Jun. 22-Jul. 02, 2015. Changes in Flood Risk and Perception in Catchments and Cities*. Book Series: Proceedings of the International Association of Hydrological Sciences (IAHS). Rogger, M, H. Aksoy, M. Kooy, et al. Eds., 370, 117-123.
- Ceccherini, G., Amezttoy, I., Hernández, C.P.R. and Moreno, C.C., 2015. High-resolution precipitation datasets in South America and West Africa based on satellite-derived rainfall, enhanced vegetation index and digital elevation model. *Remote Sensing*, 7(5), 6454-6488.
- Cook, K.H. and Vizzy, E.K., 2015. The Congo Basin Walker circulation: dynamics and connections to precipitation. *Climate Dynamics*, 1-21.
- Guo, H., Bao, A., Liu, T., Chen, S. and Ndayisaba, F., 2016. Evaluation of PERSIANN-CDR for meteorological drought monitoring over China. *Remote Sensing*, 8(5), 379.
- Hagos, S.M., Leung, L.R., Yoon, J.H., Lu, J. and Gao, Y., 2016. A projection of changes in landfalling atmospheric river frequency and extreme precipitation over western North America from the Large Ensemble CESM simulations. *Geophysical Research Letters*, 43(3), 1357-1363.
- Herold, N., Alexander, L.V., Donat, M.G., Contractor, S. and Becker, A., 2016. How much does it rain over land?. *Geophysical Research Letters*, 43(1), 341-348.
- Huang, D.Q., Zhu, J., Zhang, Y.C., Huang, Y. and Kuang, X.Y., 2016. Assessment of summer monsoon precipitation derived from five reanalysis datasets over East Asia. *Quarterly Journal of the Royal Meteorological Society*, 142(694), 108-119.
- Miao, C., Sun, Q., Borthwick, A.G. and Duan, Q., 2016. Linkage between hourly precipitation events and atmospheric temperature changes over China during the warm season. *Scientific Reports*, 6, 22543.
- Osgouei, H.F., Zarghami, M. and Ashouri, H., 2016. Disaggregating radar-derived rainfall measurements in East Azarbaijan, Iran, using a spatial random-cascade model. *Theoretical and Applied Climatology, In Press*.
- Panegrossi, G., Casella, D., Dietrich, S., Marra, A.C., Sanò, P., Mugnai, A., Baldini, L., Roberto, N., Adirosi, E., Cremonini, R. and Bechini, R., 2016. Use of the GPM constellation for monitoring heavy precipitation events over the Mediterranean region. *IEEE Journal of Selected Topics in Applied Earth Observations and Remote Sensing*, 9(6), 2733-2753.
- Pfeifroth, U., Trentmann, J., Fink, A.H. and Ahrens, B., 2016. Evaluating satellite-based diurnal cycles of precipitation in the African Tropics. *Journal of Applied Meteorology and Climatology*, 55(1), 23-39.
- Prat, O.P. and Nelson, B.R., 2015. Evaluation of precipitation estimates over CONUS derived from satellite, radar, and rain gauge data sets at daily to annual scales (2002–2012). *Hydrology and Earth System Sciences*, 19(4), 2037-2056.
- Prein, A.F. and Gobiet, A., 2016. Impacts of uncertainties in European gridded precipitation observations on regional climate analysis. *International Journal of Climatology. In Press*. DOI: 10.1002/joc.4706
- Roller, C.D., Qian, J.H., Agel, L., Barlow, M. and Moron, V., 2016. Winter weather regimes in the Northeast United States. *Journal of Climate*, 29(8), 2963-2980.

- Shah, H.L. and Mishra, V., 2016. Uncertainty and bias in satellite-based precipitation estimates over Indian subcontinental basins: implications for real-time streamflow simulation and flood prediction. *Journal of Hydrometeorology*, 17(2), 615-636.
- Sharifi, E., Steinacker, R. and Saghafian, B., 2016. Assessment of GPM-IMERG and other precipitation products against gauge data under different topographic and climatic conditions in Iran: preliminary results. *Remote Sensing*, 8(2), 135.
- Sharma, B. and Smakhtin, V., 2016. Increasing early warning lead-time through improved transboundary flood forecasting in the Gash river basin, horn of Africa. In *Flood Forecasting: A Global Perspective*, 183-203. DOI: 10.1016/B978-0-12-801884-2.00008-6..
- Solmon, F., V.S. Nair, and M. Mallet, 2015. Increasing Arabian dust activity and the Indian summer monsoon. *Atmos. Chem. Phys.*, 15(14), 8051-8064.
- Tan, M.L., Ibrahim, A.L., Duan, Z., Cracknell, A.P. and Chaplot, V., 2015. Evaluation of six high-resolution satellite and ground-based precipitation products over Malaysia. *Remote Sensing*, 7(2), 1504-1528.
- Vanmaercke, M., Poesen, J., Van Mele, B., Demuzere, M., Bruynseels, A., Golosov, V., Bezerra, J.F.R., Bolysov, S., Dvinskih, A., Frankl, A. and Fuseina, Y., 2016. How fast do gully headcuts retreat?. *Earth-Science Reviews*, 154, 336-355.
- Viterbo, F., von Hardenberg, J., Provenzale, A., Molini, L., Parodi, A., Sy, O.O. and Tanelli, S., 2016. High-resolution simulations of the 2010 Pakistan flood event: sensitivity to parameterizations and initialization time. *Journal of Hydrometeorology*, 17(4), 1147-1167.
- Yang, W., John, V.O., Zhao, X., Lu, H. and Knapp, K.R., 2016. Satellite climate data records: development, applications, and societal benefits. *Remote Sensing*, 8(4), 331.
- Yang, Z., Hsu, K., Sorooshian, S., Xu, X., Braithwaite, D. and Verbist, K.M., 2016. Bias adjustment of satellite-based precipitation estimation using gauge observations: A case study in Chile. *Journal of Geophysical Research: Atmospheres*, 121(8), 3790-3806.
- Yong, B., 2015. Comments on "Error analysis of satellite precipitation products in mountainous basins". *Journal of Hydrometeorology*, 16(3), 1443-1444.
- Yong, B., Wang, J., Ren, L., You, Y., Xie, P. and Hong, Y., 2016. Evaluating four multisatellite precipitation estimates over the Diaoyu Islands during typhoon seasons. *Journal of Hydrometeorology*, 17(5), 1623-1641.
- You, Y., Wang, N.Y., Ferraro, R. and Meyers, P., 2016. A prototype precipitation retrieval algorithm over land for ATMS. *Journal of Hydrometeorology*, 17(5), 1601-1621.

## **8. Dataset and Document Revision History**

Rev 0 – 10 July 2016